Supporting Information

Azo-bridged calix[4]resorcinarene-based porous organic frameworks with highly efficient enrichment of volatile iodine

Kongzhao Su,[a] Wenjing Wang,[b] Beibei Li[a,b] and Daqiang Yuan*[a]

† State Key Laboratory of Structural Chemistry, Fujian Institute of Research on the Structure of Matter, Chinese Academy of Sciences, 155 Yangqiao Road West, Fuzhou, Fujian 350002, P. R. China; E-mail: *ydq@fjirsm.ac.cn*; Fax: +86-591-83794946; Tel: +86-591-83792460.

‡ University of Chinese Academy of Sciences, No.19(A) Yuquan Road, Shijingshan District, Beijing 100049, P. R. China.

Contents:

Experiment procedure for the uptake of iodine vapor

Iodine uptake experiments based on gravimetric measurements were measured in the following procedure. 20 mg activated CalPOFs in a small open beaker and excess iodine were placed in a sealed glass container, heated at 75 °C under ambient pressure. Some contact time later, the CalPOF sample was cooled down and weighed. The iodine uptake of CalPOF was calculated by weight gain: $\alpha = [(W_2 - W_1)/W_1] \times 100$ wt %, where α is the iodine uptake, W_1 and W_2 are the mass of CalPOF sample before and after being exposed to iodine vapor, respectively.

Kinetic models of the iodine adsorption of CalPOFs

Three different kinetic models including, namely pseudo-first-order, pseudo-second-order model and intraparticle diffusion model as following were employed to calculate the controlling mechanism of the iodine adsorption process. The linear forms of the aforementioned models can be expressed by equations 1-3, respectively.

$$\ln(q_e - q_t) = \ln q_e - k_1 t \qquad \text{(Equation 1)}$$

$$\frac{t}{q_t} = \frac{1}{k_2 q_e^2} + \frac{1}{q_e} t \qquad \text{(Equation 2)}$$

$$q_t = k_{int} t^{0.5} + C \qquad \text{(Equation 3)}$$

In these equations, q_t is amount of I_2 adsorbed (g g^{-1}) at any time t, k_1 (min^{-1}) and k_2 (g g^{-1} min^{-1}) are the pseudo-first-order and the pseudo-second-order rate constants, respectively. k^{int} (g g^{-1} $min^{-1/2}$) is the intraparticle diffusion rate constant, and C (g g^{-1}) is the constant proportional to the extent of boundary layer thickness.

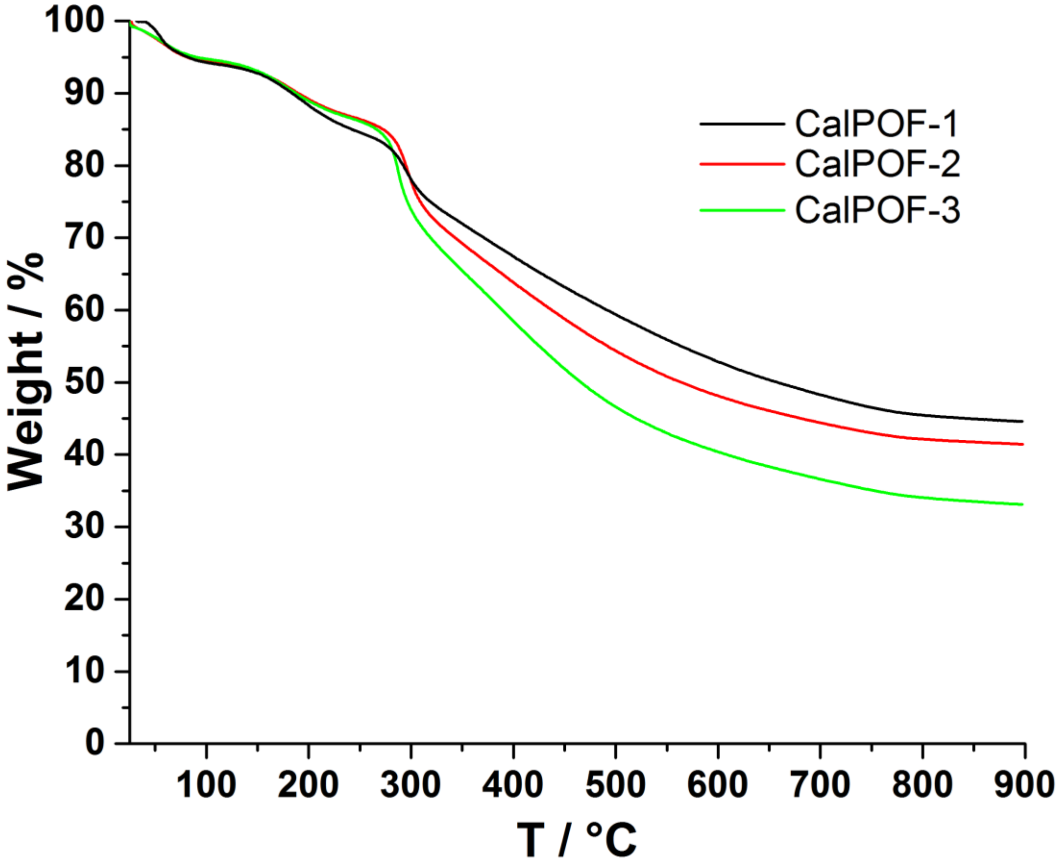

Figure S1. The TG curves of CalPOFs.

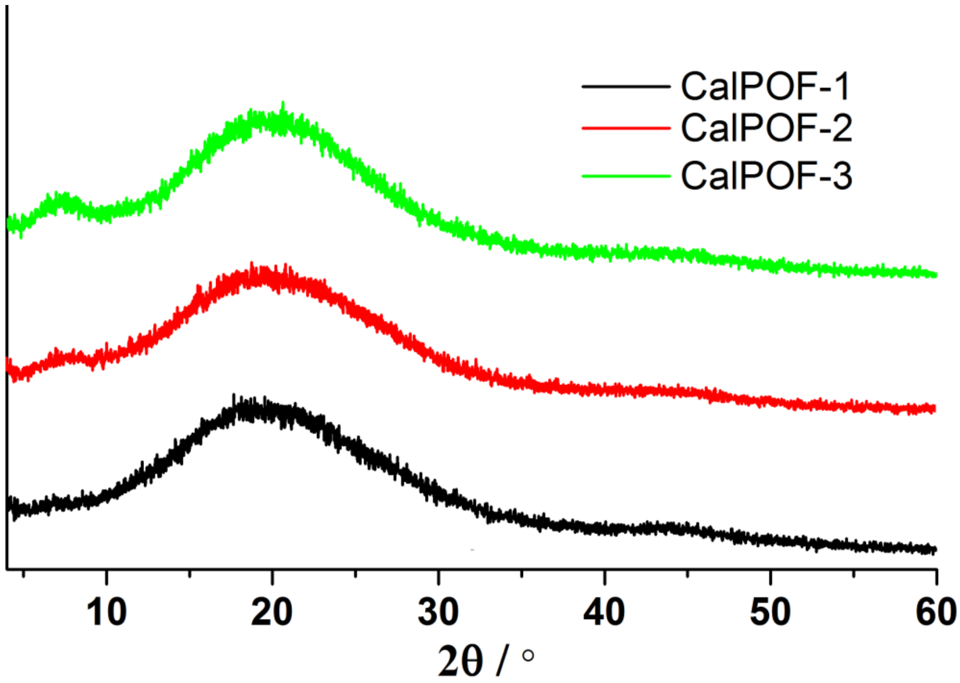

Figure S2. PXRD patterns of CalPOFs.

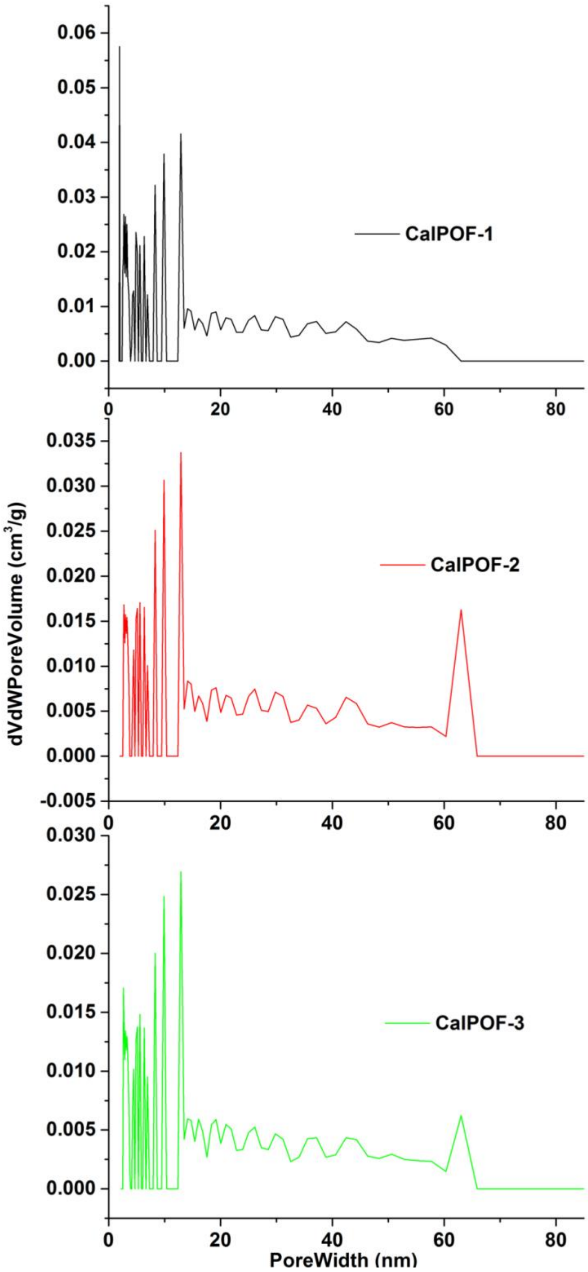

Figure S3. Pore size distribution for **CalPOF-1**, **CalPOF-2** and **CalPOF-3** calculated by NLDFT.

Table S1. Calculation of iodine sorption properties of each component.

	CalPOF-1	CalPOF-2	CalPOF-3
Azo group density	11.71%	11.06%	10.48%
RsC$_n$ unit density[a]	50.20%	47.42%	44.93%
BET / m^2 g^{-1}	303	154	91
I_2 capacity mg g^{-1}	4770	4060	3530

[a]The calculated calix[4]resorcinarene unit densities of the CalPOFs are not include the alkyl chains.

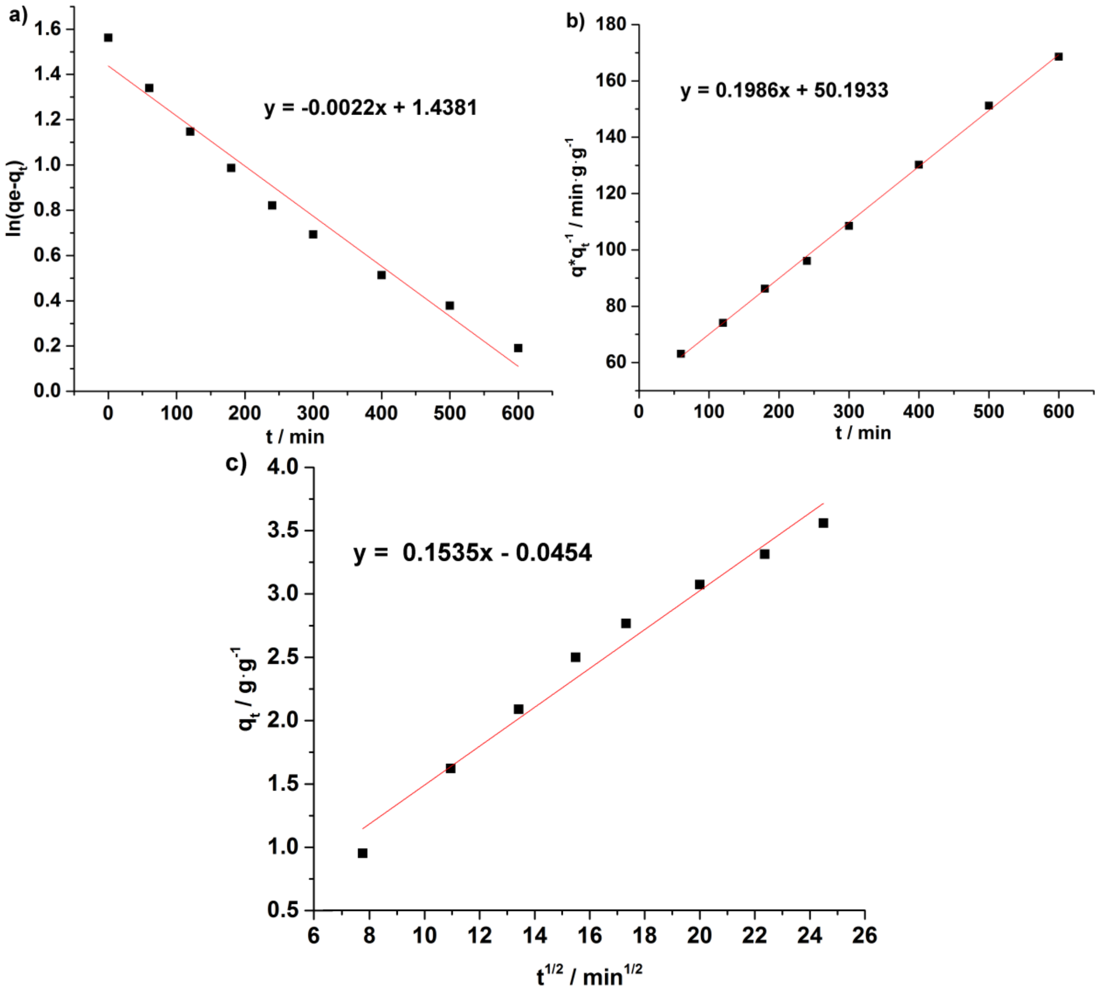

Figure S4. (a) Pseudo-first-order, (b) pseudo-second-order model, and (c) intraparticle diffusion model plots for the iodine vapor uptake into **CalPOF-1**.

Table S2. Kinetic parameters for the iodine vapor uptake into **CalPOF-1**.

q_e (exp) ($g\ g^{-1}$)	pseudo-first-order			pseudo-second-order		
	q_e ($g\ g^{-1}$)	k_1 (min^{-1})	R^2	q_e ($g\ g^{-1}$)	k_2 ($g\ g^{-1}\ min^{-1}$)	R^2
4.7725	4.2127	0.0022	0.9694	5.0352	0.0008	0.9989

intraparticle diffusion		
k_{int} ($g\ g^{-1}\ min^{-1/2}$)	C ($g\ g^{-1}$)	R^2
0.1535	0.0454	0.9735

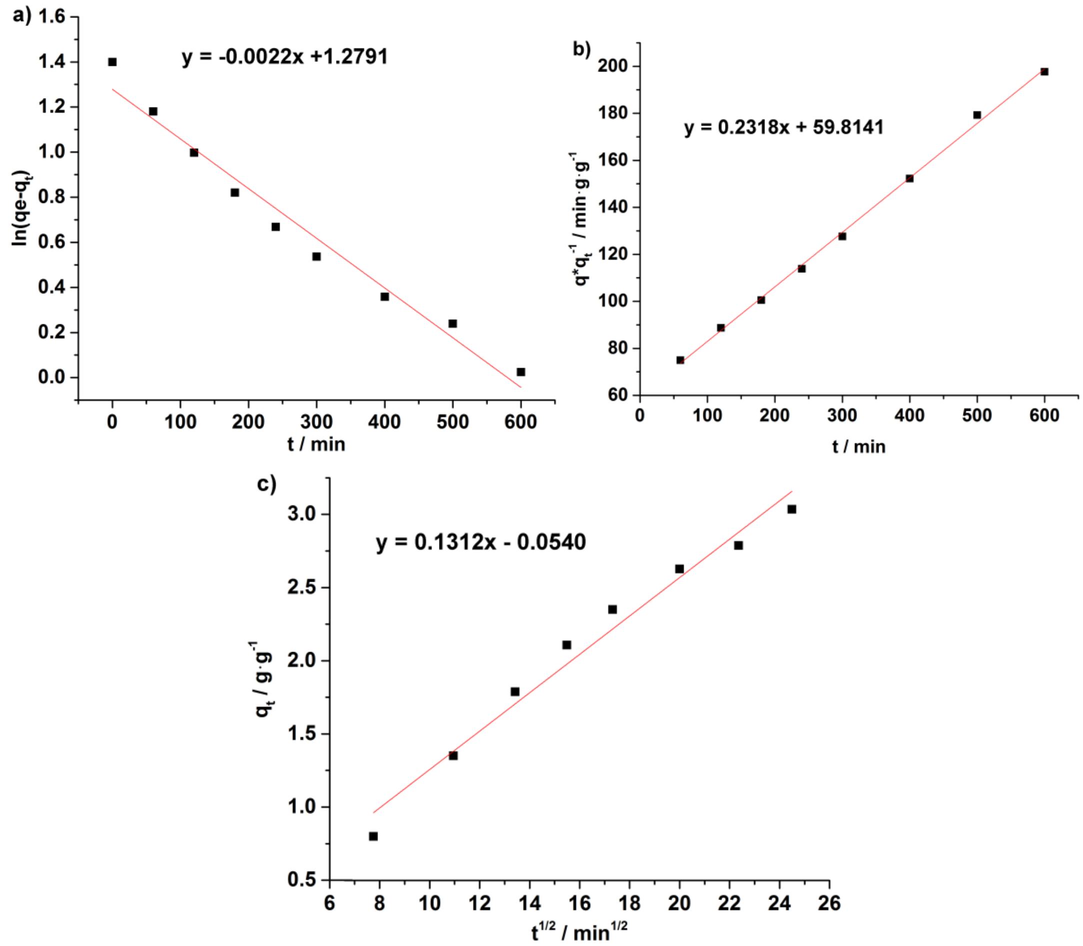

Figure S5. (a) Pseudo-first-order, (b) pseudo-second-order model, and (c) intraparticle diffusion model plots for the iodine vapor uptake into **CalPOF-2**.

Table S3. Kinetic parameters for the iodine vapor uptake into **CalPOF-2**.

q_e (exp) ($g\ g^{-1}$)	pseudo-first-order			pseudo-second-order		
	q_e ($g\ g^{-1}$)	k_1 (min^{-1})	R^2	q_e ($g\ g^{-1}$)	k_2 ($g\ g^{-1}\ min^{-1}$)	R^2
4.0618	3.5934	0.0022	0.9698	4.3141	0.0009	0.9979

intraparticle diffusion		
k_{int} ($g\ g^{-1}\ min^{-1/2}$)	C ($g\ g^{-1}$)	R^2
0.1312	0.0540	0.9725

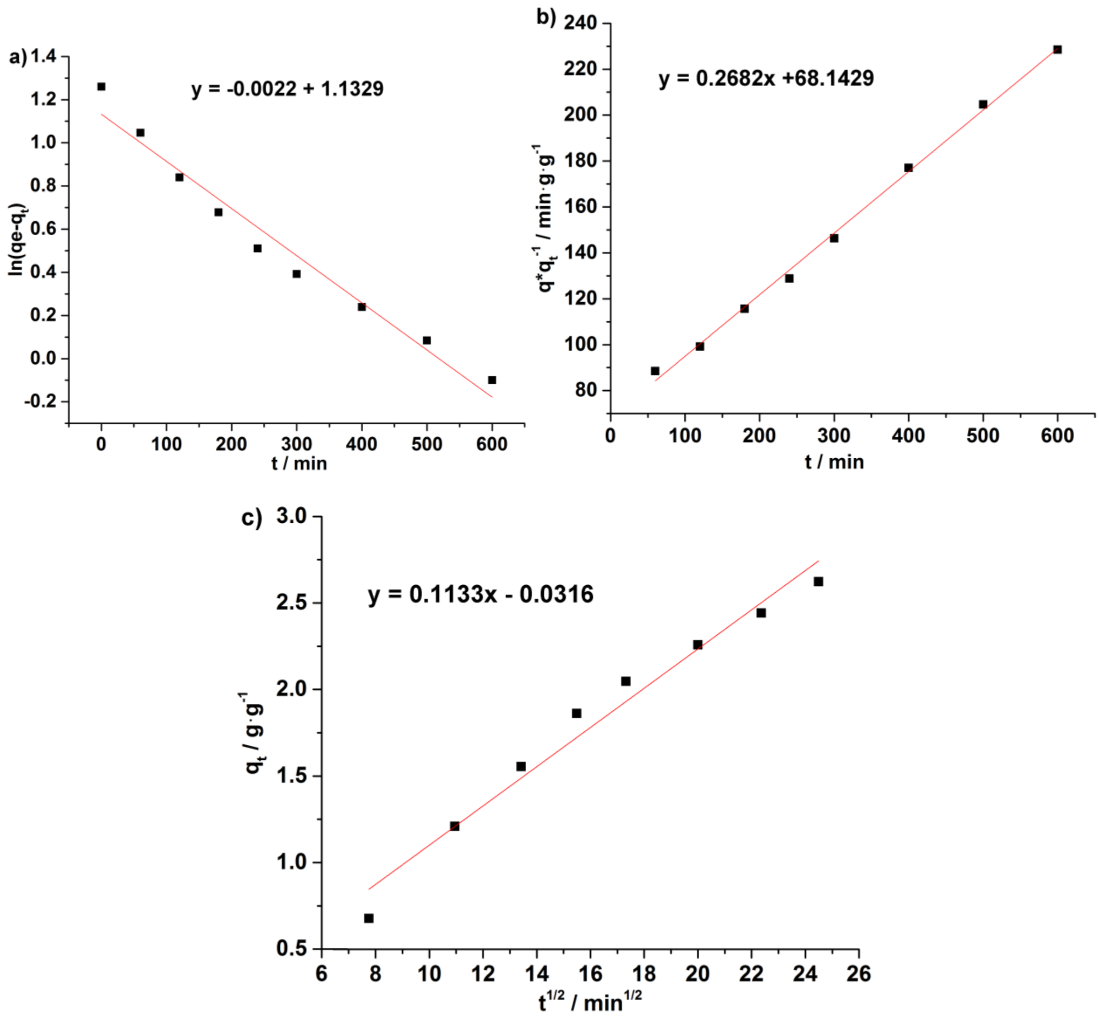

Figure S6. (a) Pseudo-first-order, (b) pseudo-second-order model, and (c) intraparticle diffusion model plots for the iodine vapor uptake into **CalPOF-2**.

Table S4. Kinetic parameters for the iodine vapor uptake into **CalPOF-3**.

q_e (exp) ($g\ g^{-1}$)	pseudo-first-order			pseudo-second-order		
	q_e ($g\ g^{-1}$)	k_1 (min^{-1})	R^2	q_e ($g\ g^{-1}$)	k_2 ($g\ g^{-1}\ min^{-1}$)	R^2
3.5297	3.1046	0.0022	0.9659	3.7286	0.0010	0.9969

intraparticle diffusion		
k_{int} ($g\ g^{-1}\ min^{-1/2}$)	C ($g\ g^{-1}$)	R^2
0.1133	-0.0316	0.9674

Table S5. Summary of iodine uptake properties of porous materials.

Adsorbent	Temperature (°C)	Pressure	S_{BET} ($m^2 g^{-1}$)	Iodine capacity (mg I_2/g)	Ref
TPT-BD COF	75	1 bar	109	5430	1
TTPAB	77	1 bar	512	4900	2
PSIF-1a	75	1 bar	320	4850	3
SIOC-COF-7	75	1 bar	618	4810	4
ETTA-TPA COF	75	1 bar	1822	4790	5
CalPOF-1	75	1 bar	303	4770	This work
COF-DL229	75	1 bar	1762	4700	6
HCP	75	1 bar	584	4600	7
TatPOP-2	75	1 bar	36.5	4500	8
TTPB	77	1 bar	222	4430	9
NDB-S	75	1 bar	56.45	4250	10
CalPOF-2	75	1 bar	154	4060	This work
TPT-DHBD COF	75	1 bar	297	4030	1
CalPOF-3	75	1 bar	91	3530	This work
SCMP-II	50	1 bar	119.76	3450	11
HCMP-3(reduced)	85	1 bar	82	3360	12
CalP4-Li	75	1 bar	445	3120	13
AzoPPN	77	1 bar	400	2900	14
BDP-CPP-1	75	1 bar	635	2830	15
PAF-24	75	1 bar	136	2760	16
MelPOP-2	75	1 bar	50.5	2620	8
Azo-Trip	77	1 bar	510	2380	17
NiMoS chalcogels	60	1 bar	490	2250	18
CalP4	75	1 bar	759	2200	13
CMPN-3	70	1 bar	1368	2030	19
NOP-54	75	1 bar	1178	2020	20

Ni-CMP	77	1 bar	2630	2020	21
NTP	75	1 bar	1067	1800	22
TTPT	77	1 bar	315.5	1770	23
Cu-BTC	75	1 bar	-	1750	24
ZIF-8	75	1 bar	1875	1200	25
Activated carbon	75	1 bar	-	300	22
Ag@Zeolite Mordenites	95	1 bar	-	275	26
Ag@Mon-POF	70	1 bar	690	250	27

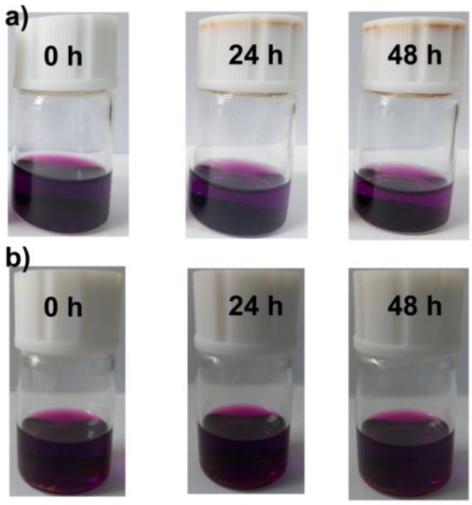

Figure S7. Photos of I_2-absorbed process of actived carbon (a) and zeolite 13X (b).

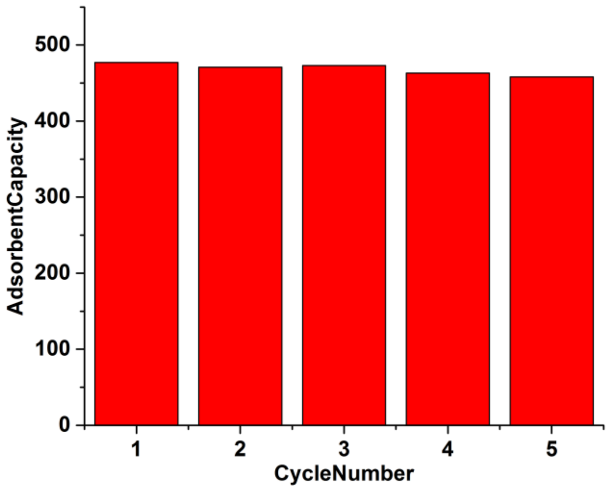

Figure S8. Recycle test of **CalPOF-1** in iodine vapor adsorption. In that case, iodine-loaded **CalPOF-1** was purified by Soxhlet extraction in ethanol for 24 h and dried in vacuum for the next iodine vapor adsorption cycle.

References

(1) Guo, X.; Tian, Y.; Zhang, M.; Li, Y.; Wen, R.; Li, X.; Li, X.; Xue, Y.; Ma, L.; Xia, C.; Li, S.: Mechanistic Insight into Hydrogen-Bond-Controlled Crystallinity and Adsorption Property of Covalent Organic Frameworks from Flexible Building Blocks. *Chem. Mater.* **2018**, *30*, 2299-2308.

(2) Geng, T.; Ye, S.; Zhu, Z.; Zhang, W.: Triazine-based conjugated microporous polymers with N,N,N′,N′-tetraphenyl-1,4-phenylenediamine, 1,3,5-tris(diphenylamino)benzene and 1,3,5-tris[(3-methylphenyl)-phenylamino]benzene as the core for high iodine capture and fluorescence sensing of o-nitrophenol. *J. Mater. Chem. A.* **2018**, *6*, 2808-2816.

(3) Janeta, M.; Bury, W.; Szafert, S.: Porous Silsesquioxane-Imine Frameworks as Highly Efficient Adsorbents for Cooperative Iodine Capture. *ACS Appl. Mat. Interfaces* **2018**, *10*, 19964-19973.

(4) Yin, Z.-J.; Xu, S.-Q.; Zhan, T.-G.; Qi, Q.-Y.; Wu, Z.-Q.; Zhao, X.: Ultrahigh volatile iodine uptake by hollow microspheres formed from a heteropore covalent organic framework. *Chem. Commun.* **2017**, *53*, 7266-7269.

(5) Wang, P.; Xu, Q.; Li, Z.; Jiang, W.; Jiang, Q.; Jiang, D.: Exceptional Iodine Capture in 2D Covalent Organic Frameworks. *Adv. Mater.* **2018**, *30*.

(6) Wang, C.; Wang, Y.; Ge, R. L.; Song, X. D.; Xing, X. Q.; Jiang, Q. K.; Lu, H.; Hao, C.; Guo, X. W.; Gao, Y. A.; Jiang, D. L.: A 3D Covalent Organic Framework with Exceptionally High Iodine Capture Capability. *Chem. Eur. J.* **2018**, *24*, 585-589.

(7) X. Li, G. Chen, J. Ma, Q. Jia, Pyrrolidinone-based hypercrosslinked polymers for reversible capture of radioactive iodine, Separation and Purification Technology (2018), doi: https://doi.org/10.1016/j.seppur. 2018.09.041.

(8) Xiong, S.; Tao, J.; Wang, Y.; Tang, J.; Liu, C.; Liu, Q.; Wang, Y.; Yu, G.; Pan, C.: Uniform poly(phosphazene–triazine) porous microspheres for highly efficient iodine removal. *Chem. Commun.* **2018**, *54*, 8450-8453.

(9) Geng, T.; Zhu, Z.; Zhang, W.; Wang, Y.: A nitrogen-rich fluorescent conjugated microporous polymer with triazine and triphenylamine units for high iodine capture and nitro aromatic compound detection. *J. Mater. Chem. A.* **2017**, *5*, 7612-7617.

(10) Guo, Z. X.; Sun, P. L.; Zhang, X.; Lin, J. B.; Shi, T.; Liu, S. F.; Sun, A. B.; Li, Z. B.: Amorphous Porous Organic Polymers Based on Schiff-Base Chemistry for Highly Efficient Iodine Capture. *Chem. Asian J.* **2018**, *13*, 2046-2053.

(11) Ren, F.; Zhu, Z.; Qian, X.; Liang, W.; Mu, P.; Sun, H.; Liu, J.; Li, A.: Novel thiophene-bearing conjugated microporous polymer honeycomb-like porous spheres with ultrahigh iodine uptake. *Chem. Commun.* **2016**, *52*, 9797-9800.

(12) Liao, Y.; Weber, J.; Mills, B. M.; Ren, Z.; Faul, C. F. J.: Highly Efficient and Reversible Iodine Capture in Hexaphenylbenzene-Based Conjugated Microporous Polymers. *Macromolecules* **2016**, *49*, 6322-6333.

(13) Shetty, D.; Raya, J.; Han, D. S.; Asfari, Z.; Olsen, J.-C.; Trabolsi, A.: Lithiated Polycalix 4 arenes for Efficient Adsorption of Iodine from Solution and Vapor Phases. *Chem. Mater.* **2017**, *29*, 8968-8972.

(14) Li, H.; Ding, X.; Han, B.-H.: Porous Azo-Bridged Porphyrin-Phthalocyanine Network with High Iodine Capture Capability. *Chem. Eur. J.* **2016**, *22*, 11863-11868.

(15) Zhu, Y.; Ji, Y.-J.; Wang, D.-G.; Zhang, Y.; Tang, H.; Jia, X.-R.; Song, M.; Yu, G.; Kuang, G.-C.: BODIPY-based conjugated porous polymers for highly efficient volatile iodine capture. *J. Mater. Chem. A.* **2017**, *5*, 6622-6629.

(16) Yan, Z.; Yuan, Y.; Tian, Y.; Zhang, D.; Zhu, G.: Highly Efficient Enrichment of Volatile Iodine by Charged Porous Aromatic Frameworks with Three Sorption Sites. *Angew. Chem. Int. Ed.* **2015**, *54*, 12733-12737.

(17) Dang, Q.-Q.; Wang, X.-M.; Zhan, Y.-F.; Zhang, X.-M.: An azo-linked porous triptycene network as an absorbent for CO2 and iodine uptake. *Polym.Chem.* **2016**, *7*, 643-647.

(18) Subrahmanyam, K. S.; Sarma, D.; Malliakas, C. D.; Polychronopoulou, K.; Riley, B. J.; Pierce, D. A.; Chun, J.; Kanatzidis, M. G.: Chalcogenide Aerogels as Sorbents for Radioactive Iodine. *Chem. Mater.* **2015**, *27*, 2619-2626.

(19) Chen, Y.; Sun, H.; Yang, R.; Wang, T.; Pei, C.; Xiang, Z.; Zhu, Z.; Liang, W.; Li, A.; Deng, W.: Synthesis of conjugated microporous polymer nanotubes with large surface areas as absorbents for iodine and CO2 uptake. *J. Mater. Chem. A.* **2015**, *3*, 87-91.

(20) Chen, D.; Fu, Y.; Yu, W.; Yu, G.; Pan, C.: Versatile Adamantane-based porous polymers with enhanced microporosity for efficient CO2 capture and iodine removal. *Chem. Eng. J.* **2018**, *334*, 900-906.

(21) A, S.; Zhang, Y.; Li, Z.; Xia, H.; Xue, M.; Liu, X.; Mu, Y.: Highly efficient and reversible iodine capture using a metalloporphyrin-based conjugated microporous polymer. *Chem. Commun.* **2014**, *50*, 8495-8498.

(22) Ma, H.; Chen, J.-J.; Tan, L.; Bu, J.-H.; Zhu, Y.; Tan, B.; Zhang, C.: Nitrogen-Rich Triptycene-Based Porous Polymer for Gas Storage and Iodine Enrichment. *Acs Macro Letters* **2016**, *5*, 1039-1043.

(23) Geng, T.; Zhang, W.; Zhu, Z.; Chen, G.; Ma, L.; Ye, S.; Niu, Q.: A covalent triazine-based framework from tetraphenylthiophene and 2,4,6-trichloro-1,3,5-triazine motifs for sensing o-nitrophenol and effective I2 uptake. *Polym. Chem.* **2018**, *9*, 777-784.

(24) Sava, D. F.; Chapman, K. W.; Rodriguez, M. A.; Greathouse, J. A.; Crozier, P. S.; Zhao, H.; Chupas, P. J.; Nenoff, T. M.: Competitive I-2 Sorption by Cu-BTC from Humid Gas Streams. *Chem. Mater.* **2013**, *25*, 2591-2596.

(25) Sava, D. F.; Garino, T. J.; Nenoff, T. M.: Iodine Confinement into Metal-Organic Frameworks (MOFs): Low-Temperature Sintering Glasses To Form Novel Glass Composite Material (GCM) Alternative Waste Forms. *Ind. Eng. Chem. Res.* **2012**, *51*, 614-620.

(26) Chapman, K. W.; Chupas, P. J.; Nenoff, T. M.: Radioactive Iodine Capture in Silver-Containing Mordenites through Nanoscale Silver Iodide Formation. *J. Am. Chem. Soc.* **2010**, *132*, 8897-+.

(27) Katsoulidis, A. P.; He, J.; Kanatzidis, M. G.: Functional Monolithic Polymeric Organic Framework Aerogel as Reducing and Hosting Media for Ag nanoparticles and Application in Capturing of Iodine Vapors. *Chem. Mater.* **2012**, *24*, 1937-1943.